Novel Aspects of the [1,3] Sigmatropic Silyl Shift in Allylsilane

Tokio Yamabe,*,†,‡ Koichi Nakamura,† Yoshihito Shiota,† Kazunari Yoshizawa,† Susumu Kawauchi,§ and Mitsuo Ishikawa||

Contribution from the Department of Molecular Engineering, Kyoto University, Sakyo-ku, Kyoto 606-01, Japan, Institute for Fundamental Chemistry, 34-4 Takano-Nishihiraki-cho, Sakyo-ku, Kyoto 606, Japan, Department of Polymer Chemistry, Tokyo Institute of Technology, Meguro-ku, Tokyo 152, Japan, and Department of Chemical Technology, Kurashiki University of Science and the Arts, Kurashiki, Okayama 712, Japan

Received July 9, 1996. Revised Manuscript Received October 23, 1996[⊗]

Abstract: *Ab initio* molecular orbital calculations of the C═CCSi torsion and the [1,3] sigmatropic silyl shift in allylsilane (SiC_3H_8, **1**) have been carried out. It is clarified that the *skew* conformer of **1** is more stable than other conformers. Its torsional energy depends on the $\sigma-\pi$ hyperconjugation as compared with that of 1-butene (**2**). In the [1,3] silyl shift, the reaction coordinate of the silyl-group migration in the early and final stages is congruent with that of the C═CCSi torsion near the *skew* conformer. Divergence points on the inversion and retention paths are discussed from the viewpoint of the degree of nonplanarity of the migrating silyl group. The activation energy along the retention path is calculated to be lower than that along the inversion path at various levels of theory, which is in remarkable contrast to **2**, in which the inversion path is more favorable. From the energetical viewpoint, the [1,3] shift of the silyl group is expected to proceed with retention of the silicon configuration at the migrating center. Although this looks like an exception to the Woodward−Hoffmann rules, this may be caused by the nearly degenerate HOMO and (HOMO−1) in the transition state on the inversion path in **1**.

Introduction

The chemistry of silicon compounds is nowadays one of the most attractive themes in both academic and industrial fields of chemical research. In particular, the use of organosilicon compounds a reagents and intermediates has been of considerable importance in the synthesis of organic compounds. Allylsilanes react with a wide range of carbon electrophiles, to form carbon−carbon bonds with a high degree of regioselectivity. Allylsilanes have been studied extensively and applied to organic synthesis as species with practical synthetic utility.[1,2]

Several experimental[3] and computational[4] investigations about the structure and conformational preference of SiC_3H_8 (**1**), the simplest member of the allylsilanes, have been performed. It has been found that a nearly *skew* conformer is the most stable structure[3,4] in **1** just as in 1-butene (**2**).[5,6] However, a clear difference in the stability of the *cis* conformers of **1** and **2** has been observed.[5,6] The *cis* form of **2** is one of its stable structures, while the *cis* form of **1** is in an energy maximum. This difference between these molecules has been examined in terms of both $\sigma-\pi$ conjugation and hyperconjugation effects.[4,7,8]

Scheme 1

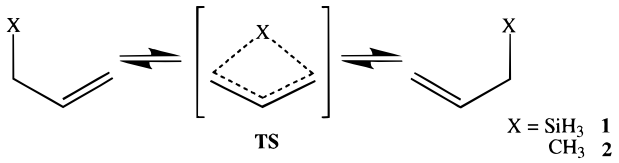

The rearrangement of allylsilanes can proceed only at relatively high temperatures by [1,3] silyl migration.[9] The reagent and product are, of course, identical in **1** and **2**, as indicated in Scheme 1. This type of intramolecular rearrangement is called sigmatropic reaction. The study of sigmatropic rearrangement has been one of the main themes in quantum chemistry. The stereochemistry of these reactions is explained systematically by the well-established Woodward−Hoffmann (W−H) rules, the basis of which is orbital symmetry.[10] These rules have been confirmed for many reactions using *ab initio* molecular orbital methods of various levels of theory.[11] According to this rule, the thermal and suprafacial [1,3] rearrange-

† Kyoto University.
‡ Institute for Fundamental Chemistry.
§ Tokyo Institute of Technology.
|| Kurashiki University of Science and the Arts.
⊗ Abstract published in *Advance ACS Abstracts,* January 1, 1997.

(1) (a) Sarker, T. K.; Anderson, N. H. *Tetrahedron Lett*. **1978**, 3513. (b) Fleming, I.; Paterson, I. *Synthesis* **1979**, 446. (c) Chan, T. H.; Fleming, I. *Ibid*. **1979**, 761. (d) Colvin, E. W. *Silicon in Organic Synthesis*; Butterworth: Glasgow, 1981. (e) Sakurai, H. *Pure Appl. Chem*. **1982**, *54*, 1. (f) Denmark, S. E.; Weber, E. J. *Helv. Chim. Acta* **1983**, *66*, 1655. (g) Sakurai, H. *Synlett* **1989**, *1*, 1. (h) Hosomi, A.; Kohra, S.; Ogata, K.; Yanagi, T.; Tominaga, Y. *J. Org. Chem*. **1990**, *55*, 2415. (i) Kira, M.; Sato, K.; Sakurai, H. *J. Am. Chem. Soc*. **1990**, *112*, 257. (j) Kira, M.; Sato, K.; Sakurai, H.; Hada, M.; Izawa, M.; Ushio, J. *Chem. Lett*. **1991**, 387. (k) Myers, A. G.; Kephart, S. E.; Chen, H. *J. Am. Chem. Soc*. **1992**, *114*, 7922. (l) Denmark, S. E.; Griedel, B. D.; Coe, D. M. *J. Org. Chem*. **1993**, *58*, 988. (m) Denmark, S. E.; Griedel, B. E.; Coe, D. M.; Schnute, M. E. *J. Am. Chem. Soc*. **1994**, *116*, 7026.

(2) Matsumoto, K.; Oshima, K.; Uchimoto, K. *J. Org. Chem*. **1994**, *59*, 712.

(3) (a) Hayashi, M.; Imachi, M.; Saito, M. *Chem. Lett*. **1977**, 221. (b) Ohno, K.; Taga, K.; Murata, H. *Bull. Chem. Soc. Jpn*. **1977**, *50*, 2870.

(4) Profeta, S., Jr.; Unwalla, R. J.; Cartledge, F. K. *J. Org. Chem*. **1986**, *51*, 1884.

(5) (a) Kondo, S.; Hirota, E.; Morino, Y. *J. Mol. Spectrosc*. **1968**, *28*, 471. (b) Durig, J. R.; Compton, D. A. C. *J. Phys. Chem*. **1980**, *84*, 773.

(6) Wiberg, K. B.; Martin, E. *J. Am. Chem. Soc*. **1985**, *107*, 5035.

(7) *Carbon-Functional Organosilicon Compounds*; Chavalovský, V., Bellama, J. M., Eds.; Plenum Press: New York, 1984.

(8) Egorochkin, A. N. *Russ. Chem. Rev*. **1984**, *53*, 445.

(9) (a) Kwart, H.; Slutsky, J. *J. Am. Chem. Soc*. **1972**, *94*, 2515. (b) Slutsky, J.; Kwart, H. *Ibid*. **1973**, *95*, 8678.

(10) (a) Hoffmann, R.; Woodward, R. B. *J. Am. Chem. Soc*. **1965**, *87*, 395. (b) Woodward, R. B.; Hoffmann, R. *Ibid*. **1965**, *87*, 2046. (c) Hoffmann, R.; Woodward, R. B. *Ibid*. **1965**, *87*, 2511. (d) Woodward, R. B.; Hoffmann, R. *Ibid*. **1965**, *87*, 4389. (e) Woodward, R. B.; Hoffmann, R. *Angew. Chem., Int. Ed. Engl*. **1969**, *8*, 781. (f) Woodward, R. B.; Hoffmann, R. *The Conservation of Orbital Symmetry*; Verlag Chemie: Weinheim, 1970.

(11) (a) Houk, K. N.; Li, Y.; Evanseck, J. D. *Angew. Chem., Int. Ed. Engl*. **1992**, *31*, 682. (b) Bernardi, F.; Olivucci, M.; Robb, M. A.; Tonachini, G. *J. Am. Chem. Soc*. **1992**, *114*, 5805.

S0002-7863(96)02352-9 CCC: $14.00

Table 1. Calculated Relative Energies and Dihedral Angles of Allylsilane and 1-Butene Conformers

	allylsilane (**1**)						1-butene (**2**) RHF/6-31G**	
	RHF/3-21G*		RHF/6-31G**		MP2(full)/6-31G**			
	ΔE^a	ϕ^b	ΔE^a	ϕ^b	ΔE^a	ϕ^b	ΔE^a	ϕ^b
local minimum	2.2	0.0	2.1	0.0			0.7	0.0
local maximum	2.3	21.9	2.3	32.7	2.3	0.0	2.5	54.3
local minimum	0	101.8	0	106.9	0	103.7	0	119.8
local maximum	3.5	180.0	3.5	180.0	3.7	180.0	2.2	180.0

[a] In units of kilocalories/mole. [b] In units of degree.

Scheme 2

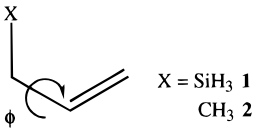

ments of methyl occur with inversion of configuration at the migrating center in a process involving the antisymmetric 2p orbital of the methyl carbon.

Although the W−H rules correctly predict the stereoselection in the reactions of organic compounds with a carbon framework, it is of great interest to look at whether this rule is applicable to the stereoselection of organosilicon compounds as well as other heteroatomic systems. In 1973, Slutsky and Kwart[9] reported the observation of unimolecular gas-phase silaallylic rearrangement in optically active α-naphthylphenylmethylallylsilane. They concluded that this migration proceeds with inversion of the silicon configuration. On the other hand, retention of configuration at the migrating silicon center was identified for the [1,3] shift of β-keto silanes by Brook et al.[12] and that of mono-*O*-silyl enols of β-dicarbonyl compounds by Kusnezowa et al.[13] A recent *ab initio* study by Takahashi and Kira[14] has suggested that the retention path is more favorable than the inversion path in the [1,3] silyl shift in allylsilane. However, the stereochemistry of organosilicon compounds is still not clear at present. To our knowledge, there have been few theoretical studies on the sigmatropic reaction of silicon compounds, except for ref 14.

In this context, we have carried out *ab initio* molecular orbital calculations concerning the energy barrier of internal rotation about the C−C single bond adjacent to the C═C double bond of allylsilane, as indicated in Scheme 2. Moreover, we have analyzed two transition states (TSs) of an inversion path (**TS1a**) and a retention path (**TS1b**) in the sigmatropic rearrangement ([1,3] silyl shift). On the basis of intrinsic reaction coordinate (IRC)[15] analyses, we consider in detail the stereochemistry and the mechanism of the [1,3] sigmatropic silyl shift in allylsilane (**1**).

Method of Calculation

All molecular orbital calculations were performed with Gaussian 92 and 94 *ab initio* programs.[16,17] Conformational minima and maxima of allylsilane (**1**) along the internal rotation around the C−C single bond were optimized with the 3−21G* [18] and 6-31G** [19] basis sets and with the second-order Møller−Plesset perturbational treatment[20] (MP2(full)/6-31G**). Analytical vibrational frequencies were computed to ensure that each conformer corresponds to a true minimum (no negative eigenvalue) or a conformational maximum (one imaginary frequency along the C−C rotation). Relative energies as a function of C═CCSi torsional angle were calculated every 10° at the RHF/6-31G** level. The critical points of 1-butene (**2**) along the C−C rotation are also computed at the RHF/6-31G** level.

Furthermore, we carried out geometry optimizations at the RHF/6-31G** and MP2(full)/6-31G** levels for the two transition states, **TS1a** on the inversion path and **TS1b** on the retention path, in the course of the [1,3] sigmatropic silyl shift. Single-point calculations for the two TSs were performed at the CAS(4,4)/6-31G**//MP2(full)/6-31G** level.[21] Moreover, SDCI (single and double excitation configuration interactions) calculations were carried out for these TSs. We confirmed the MP2 geometries to correspond to a real TS, which should have one imaginary frequency, on the basis of analytical vibrational frequency analysis. In accord with a comment of one of the reviewers of this paper, we carried out more sophisticated geometry optimizations and numerical vibrational analyses for the two TSs at the CAS(4,4)/6-31G** level and single-point calculations at the CAS(4,4)MP2(full)/6-31G**//CAS(4,4)/6-31G** level. IRCs[15] were calculated at the RHF/6-31G** level in a mass-weighted internal coordinate system using the Gonzalez−Schlegel method[22] available in the Gaussian 92 program.[16]

Results and Discussion

Conformational Preference. Relative energies and dihedral angles ϕ, indicated in Scheme 2, at the conformational minima and maxima of **1** and **2** are listed in Table 1. Geometries for the *skew* conformers of **1** and **2**, optimized at the MP2 level, are shown in Figure 1. These two conformers are, of course, very similar in geometry, except for the C−Si and Si−H bonds. The *skew* conformers of **1** and **2** with a C═CCX dihedral angle ϕ of 103.7° and 117.7°, respectively, were confirmed to be much more stable than other conformers, where X is Si or C.

(12) Brook, A. G.; MacRae, D. M.; Limburg, W. W. *J. Am. Chem. Soc.* **1967**, *89*, 5493.
(13) Kusnezowa, A.; Ruhlmann, K. R.; Grundemann, E. *J. Organomet. Chem.* **1973**, *47*, 53.
(14) (a) Takahashi, M.; Kira, M. *Proc. Symp. Organomet. Chem. Jpn., 10th* **1993**, 205−207. (b) Takahashi, M.; Kira, M. *J. Am. Chem. Soc.*, submitted.
(15) (a) Fukui, K. *J. Phys. Chem.* **1970**, *74*, 4161. (b) Fukui, K.; Kato, S.; Fujimoto, H. *J. Am. Chem. Soc.* **1975**, *97*, 1. (c) Kato, S.; Fukui, K. *Ibid.* **1976**, *98*, 6395.
(16) Frisch, M. J.; Trucks, G. W.; Head-Gordon, M.; Gill, W. P. M.; Wong, M. W.; Foresman, J. B.; Johnson, B. G.; Schlegel, H. B.; Robb, M. A.; Replogle, E. S.; Gomperts, R.; Andres, J. L.; Raghavachari, K.; Binkley, J. S.; Gonzalez, C.; Martin, R. L.; Fox, D. J.; Defrees, D. J.; Baker, J.; Stewart, J. J. P.; Pople, J. A. *Gaussian 92*; Gaussian Inc.: Pittsburgh, PA, 1992.
(17) Frisch, M. J.; Trucks, G. W.; Schlegel, H. B.; Gill, W. P. M.; Johnson, B. G.; Robb, M. A.; Cheeseman, J. R.; Keith, T. A.; Patterson, G. A.; Montgomery, J. A.; Raghavachari, K.; Al-Laham, M. A.; Zakrzewski, V. G.; Ortiz, J. V.; Foresman, J. B.; Cioslowski, J.; Stefanov, B. B.; Nanayakkara, A.; Challacombe, M.; Peng, C. Y.; Ayala, P. Y.; Chen, W.; Wong, M. W.; Andres, J. L.; Replogle, E. S.; Gomperts, R.; Martin, R. L.; Fox, D. J.; Binkley, J. S.; Defrees, D. J.; Baker, J.; Stewart, J. J. P.; Head-Gordon, M.; Gonzalez, C.; Pople, J. A. *Gaussian 94*; Gaussian Inc.: Pittsburgh, PA, 1995.
(18) (a) Binkley, J. S.; Pople, J. A.; Hehre, W. J. *J. Am. Chem. Soc.* **1980**, *102*, 939. (b) Gordon, M. S.; Binkley, J. S.; Pople, J. A.; Pietro, W. J.; Hehre, W. J. *Ibid.* **1982**, *104*, 2797. (c) Pietro, W. J.; Francl, M. M.; Hehre, W. J.; Defrees, D. J.; Pople, J. A.; Binkley, J. S. *Ibid.* **1982**, *104*, 5039.
(19) (a) Hehre, W. J.; Ditchfield, R.; Pople, J. A. *J. Chem. Phys.* **1972**, *56*, 2257. (b) Hariharan, P. C.; Pople, J. A. *Theor. Chim. Acta* **1973**, *28*, 213. (c) Gordon, M. S. *Chem. Phys. Lett.* **1980**, *76*, 163.
(20) Møller, C.; Plesset, M. S. *Phys. Rev.* **1934**, *46*, 618.
(21) (a) Hegarty, D.; Robb, M. A. *Mol. Phys.* **1979**, *38*, 1795. (b) Eade, R. H. E.; Robb, M. A. *Chem. Phys. Lett.* **1981**, *83*, 362.
(22) (a) Gonzalez, C.; Schlegel, H. B. *J. Chem. Phys.* **1989**, *90*, 2154. (b) Gonzalez, C.; Schlegel, H. B. *J. Phys. Chem.* **1990**, *94*, 5523. (c) Gonzalez, C.; Schlegel, H. B. *J. Chem. Phys.* **1991**, *95*, 5853.

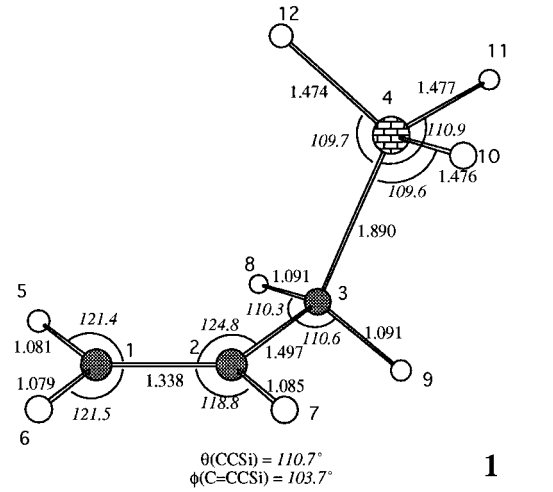

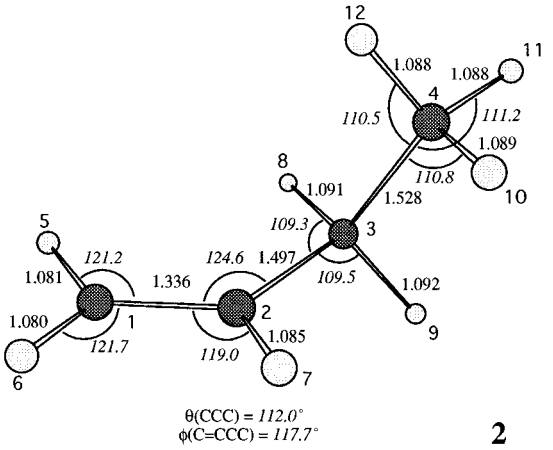

Figure 1. Geometries of the *skew* conformer of allylsilane (**1**) and 1-butene (**2**) calculated at the MP2(full)/6-31G** level. All bond lengths are in angstroms and angles (italic) are in degrees.

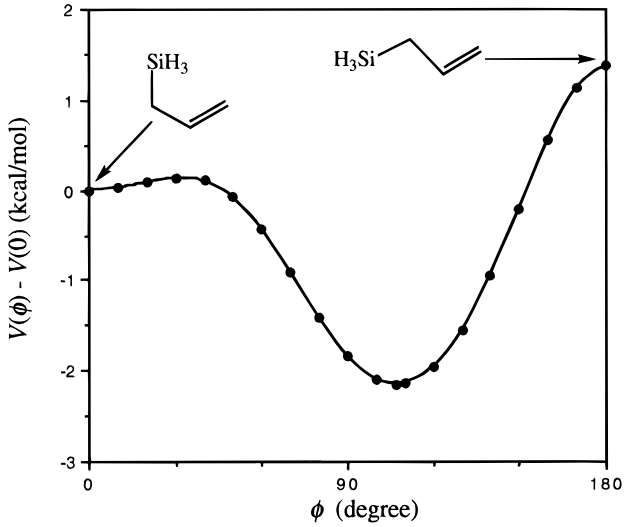

Figure 2. Torsional barrier for allylsilane (**1**) calculated at the RHF/6-31G** level. The curve follows eq 1, and the dots are values from RHF calculations.

Vibrational analyses show that these skew conformers are in a minimum on a potential energy hypersurface. The lowest vibrational mode in the *skew* conformers corresponds to the C═CCX torsional motion.

Figures 2 and 3 show the relative energies for **1** and **2** as functions of torsional angle, respectively. In contrast to the results from MM2 calculations,[4] the potential near the *cis*

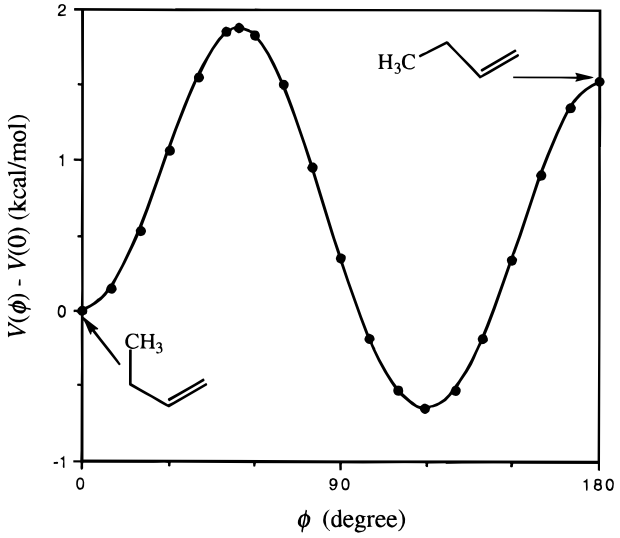

Figure 3. Torsional barrier for 1-butene (**2**) calculated at the RHF/6-31G** level. The curve follows eq 1, and the dots are values from RHF calculations.

Table 2. Fourier Coefficient of Torsional Barriers in Allylsilane and 1-Butene (kcal/mol)

	allylsilane	1-butene
V_1	−0.116	−0.348
V_2	−1.288	0.152
V_3	0.745	1.109

conformer of **1** is clearly shallow at the Hartree−Fock level of calculation. The energy barrier from the *cis* to *skew* conformers of **1** obtained from the RHF method is 0.04 kcal/mol (3-21G*) and 0.14 kcal/mol (6-31G**). At the MP2(full) level of calculation, in the end, the *cis* conformer was confirmed to be a saddle point on the potential energy surface along the C−C rotation.

We have performed a numerical treatment of the C═CCSi and C═CCC torsional energies $V(\phi)$, to expand them into the Fourier series, or to decompose them into 1-fold, 2-fold, 3-fold, and higher-order terms:[6,7,23−25]

$$V(\phi) = \sum_{n=1} \frac{V_n(1 - \cos n\phi)}{2} + V(0) \qquad (1)$$

The first three expansion coefficients corresponding to $n = 1$, 2, and 3 in eq 1 are listed in Table 2. The simulated curves as well as the points calculated at the RHF/6-31G** level for **1** and **2** are shown in Figures 2 and 3, respectively. The terms higher than 3-fold ($n \geq 4$) are approximately 0, so that the higher-order terms can be ignored. These simulations are successful.

Let us consider the physical meaning of each term appearing in eq 1. The first term ($n = 1$) is mainly regarded as an expression of methylene−X (X = silyl or methyl group) repulsion because this term destabilizes the torsional energy at $\phi = 0°$ and stabilizes it at $\phi = 180°$ for a negative V_1 (expansion coefficient) value. On the other hand, the second term ($n = 2$) stabilizes the torsional energy at $\phi = 90°$ for a negative V_2 value. Thus, this stabilization is supposed to correspond to the $\sigma-\pi$

(23) Schaefer, T.; Sebastian, R.; Penner, G. H. *Can. J. Chem.* **1991**, *69*, 496.
(24) Radom, L.; Hehre, W. J.; Pople, J. A. *J. Am. Chem. Soc.* **1972**, *94*, 2371.
(25) (a) Ponec, R.; Dejmek, L.; Chavalovský, V. *Collect. Czech. Chem. Commun.* **1980**, *45*, 2895. (b) Dejmek, L.; Ponec, R.; Chavalovský, V. *Ibid.* **1980**, *45*, 3510.

Scheme 3

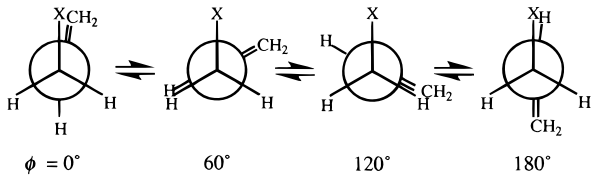

hyperconjugation effect of the perpendicular conformation[23,26] to the allyl π plane.

The third term ($n = 3$) is mainly regarded as an expression of the repulsion coming from the hydrogen−hydrogen or hydrogen−X eclipsed conformation[6,24] because this term destabilizes the torsional energy at $\phi = 60°$ and 180° for a positive V_3 value. The correction with respect to the difference in the degree of instability between the hydrogen−hydrogen eclipsed conformation and the hydrogen−X one would be included implicitly in the first term. As a consequence, we can suppose that the first and third terms in eq 1 represent a quantity of the eclipsed barriers,[6,24] as illustrated in Scheme 3.

The contribution from $\sigma-\pi$ hyperconjugation can be estimated quantitatively from the magnitude of V_2, as mentioned above. As shown in Table 2, the amplitude of V_2 of **1** is much larger than that of **2**, which is nearly 0. In addition, the magnitude of V_2 is larger than the magnitudes of V_1 and V_3 in **1** whereas the magnitude of V_2 is smaller than the magnitudes of V_1 and V_3 in **2**. These results suggest (1) that the stability from the $\sigma-\pi$ hyperconjugation with the C−Si bond in the plane perpendicular to the allyl plane is much more determining than the C−C bond[8,23] and (2) that most of the torsional energy of **1** is controlled by the $\sigma-\pi$ hyperconjugation.

Transition States of the [1,3] Silyl Shift. We next consider two types of transition states on different paths about the [1,3] silyl migration in **1**. The geometries for **TS1a** on the inversion path and **TS1b** on the retention path were optimized with the MP2(full)/6-31G** method, as shown in Figure 4. These structures hold C_s symmetry. We can see in these illustrations that the migrating silyl group is planar in **TS1a** on the inversion path while it is trigonal pyramidal in **TS1b** on the retention path. Note that the Si−C distances of 2.254 and 2.261 Å for **TS1a** and **TS1b**, respectively, are nearly equal. The geometries optimized at the CAS(4,4)/6-31G** level, not shown here, are quite similar to those shown in Figure 4. The imaginary frequencies of **TS1a** and **TS1b** are 619.2i and 478.2i cm^{-1}, respectively, at the MP2(full)/6-31G** level; however, those obtained numerically at the CAS(4,4)/6-31G** level are 660.6i and 321.3i cm^{-1}.

As shown in Table 3, the activation energy (E_a) of the [1,3] silyl migration in **1**, indicated in Scheme 1, is 62.6 kcal/mol along the inversion path and 51.8 kcal/mol along the retention path at the MP2(full)/6-31G** level, taking zero point energy (ZPE) corrections into consideration. Interestingly, the activation energy along the retention path is 10.8 kcal/mol lower than that along the inversion path. This result is not significantly changed in higher-order calculations. CASSCF calculations using the MP2(full)/6-31G** geometries show that the activation energy along the retention path is 5.2 kcal/mol lower, and SDCI calculations also favor the retention path by 11.3 kcal/mol at the same level of basis set. Moreover, CAS(4,4)/6-31G**//CAS(4,4)/6-31G** and single-point CAS(4,4)MP2(full)/6-31G** calculations at the CAS(4,4)/6-31G** geometries showed

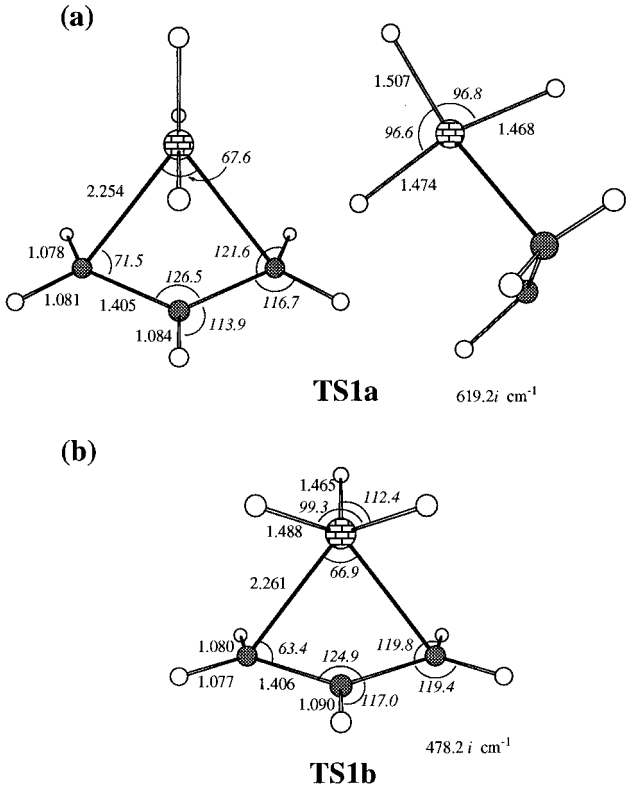

Figure 4. Calculated MP2(full)/6-31G** geometries and imaginary frequencies of the two transition states of allylsilane. (a) Inversion-path TS (**TS1a**) and (b) retention-path TS (**TS1b**). All bond lengths are in angstroms and angles (italic) are in degrees.

Table 3. Activation Energies (E_a) of Transition States of the [1,3] Silyl Shift in Allylsilane (kcal/mol) at Various Levels of Theory

	E_a		
	TS1a	**TS1b**	ΔE_a
RHF/6-31G**//RHF/6-31G**	74.0	63.2	10.8
MP2(full)/6-31G**//MP2(full)/6-31G**	62.6	51.8	10.8
CAS(4,4)/6-31G**//MP2(full)/6-31G**			5.2
SDCI/6-31G**//MP2(full)/6-31G**			11.3
CAS(4,4)/6-31G**//CAS(4,4)/6-31G**			13.9
CAS(4,4)MP2(full)/6-31G**//CAS(4,4)/6-31G**			16.1

that the retention path is also more favorable by 13.9 and 16.1 kcal/mol, respectively, as shown in Table 3. Thus, we believe that this result will not be turned over by more accurate calculations. The inconsistency between our calculational results and experiments by Slutsky and Kwart[9] may be ascribed to a substituent effect, as suggested by Takahashi and Kira.[14]

From the energetical viewpoint, the retention path is preferred compared with the inversion path in this organosilicon compound at all the levels of theory used in this study. This calculational result does not seem to be consistent with a prediction from the W−H rules. In any case, it is essential to note that two different types of transition states with comparable activation energies coexist on a potential energy hypersurface. This is in a remarkable contrast to the result for a carbon-based system **2** in which the activation energy along the inversion path is 10.3 kcal/mol smaller that that along the retention path at the CAS(4,4)/6-31G**//MP2(full)/6-31G** level, which is consistent with the W−H rule. Our main concern in this article is in the contrast between the stereoselections of the intramolecular migration in **1** and **2**.

To look in detail at the stereoselection of organosilicon compounds, let us next analyze the reaction coordinate of this rearrangement. The potential energies along the two IRCs (s)

(26) (a) Hoffmann, R.; Radom, L.; Pople, J. A.; Schleyer, P. v. R.; Hehre, W. J.; Salem, L. *J. Am. Chem. Soc.* **1972**, *94*, 6221. (b) Ponec, R.; Chavalovský, V.; Tschernyschev, E. A.; Komarenkova, N. G.; Bashkirova, S. A. *Collect. Czech. Chem. Commun.* **1974**, *39*, 1177.

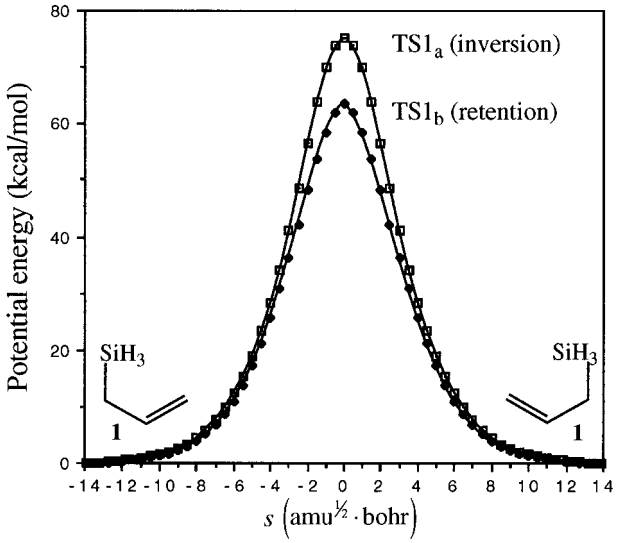

Figure 5. Potential energies along the IRC at the RHF/6-31G** level for (a) inversion and (b) retention paths.

of the inversion and retention paths calculated at the RHF/6-31G** level are shown in Figure 5. It is important to note again that in **1** the retention path has a lower activation energy than the inversion path. In contrast, the activation energies for the inversion and retention paths in a carbon-based system **2** are 72.8 and 83.1 kcal/mol, respectively, at the CAS(4,4)/6-31G**//MP2(full)/6-31G** level. Since CASSCF calculations are necessary to obtain correct results in the TSs of **2**, it is difficult to carry out IRC analyses for **2**.[27]

Putting $s = 0$ at each TS in units of amu$^{1/2}$·bohr, both IRCs lead to the reactant and product, *i.e.*, the *skew* conformer of **1**, at $s = \pm 14$. Important atomic distances along the two IRCs are shown in Figure 6. These values are, of course, symmetrical with respect to $s = 0$ since the reactant and product are identical in these systems.

In the vicinity of the reactant and product, the atomic distances and bond angles between the atoms making a chemical bond are constant. Furthermore, r_{24}, the distance between the central carbon atom of allyl and the silicon atom of migrating silyl, is also constant near the reactant and product because r_{24} can be expressed only by constant values as

$$r_{24} = \sqrt{r_{12}^2 + r_{14}^2 - 2r_{12}r_{14}\cos\theta_{214}} = \sqrt{r_{23}^2 + r_{34}^2 - 2r_{23}r_{34}\cos\theta_{234}}$$

Thus, θ_{124} and θ_{324} are also constant near the reactant and product, respectively, as expressed by

$$\sin\theta_{124} = \frac{r_{14}}{r_{24}}\sin\theta_{214}, \quad \sin\theta_{324} = \frac{r_{34}}{r_{24}}\sin\theta_{234}$$

In contrast to the atomic distances and bond angles, the change in the dihedral angle ϕ is monotonical along the IRC although the bond and dihedral angles are not shown explicitly. Consequently, in both the early and final stages of the reaction, the dihedral angle is regarded as a function of the reaction coordinate, *i.e.*, $\phi = \phi[s]$. The effect on the potential energy with a change in dihedral angle near the reactant and product can be estimated by using eq 1. Hence we calculated a C═CCSi

(27) It is well-known that the TS structures of 1-butene (**2**) cannot correctly be described by a single Slater determinant. In fact, MP2(full)/6-31G** calculations gave an erroneous result that the retention path is more favorable in **2**. The preference for the inversion path in **2** was described correctly by CAS(4,4)/6-31G**//MP2(full)/6-31G** calculations.

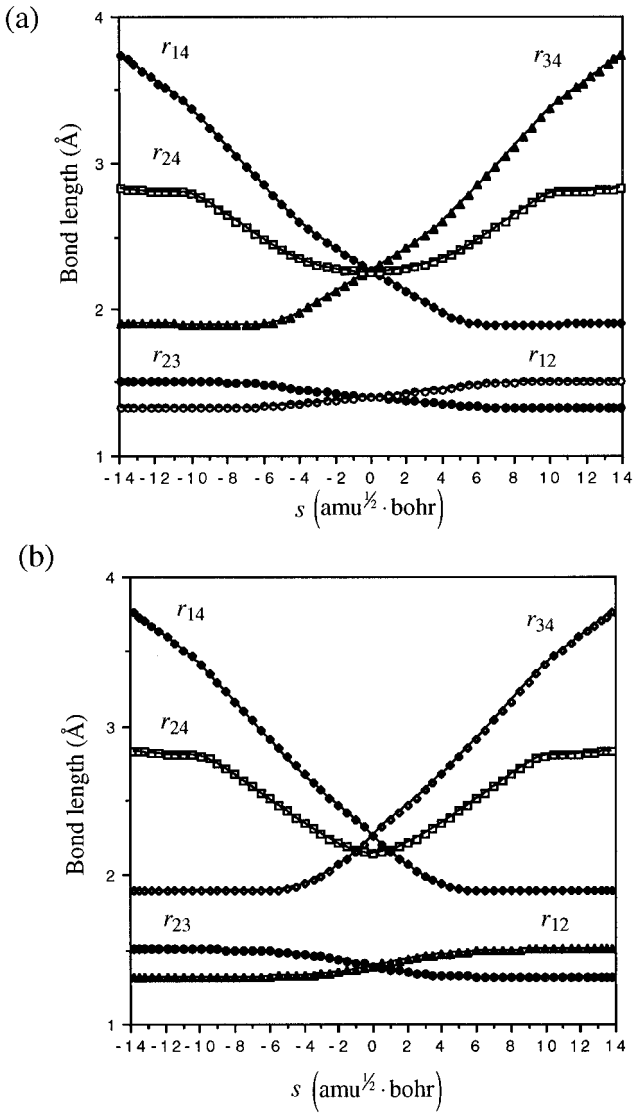

Figure 6. Atomic distances along the IRC of (a) inversion and (b) retention paths.

torsional segment of the potential energy on the IRC:

$$V'(s) = V(\phi[s]) \tag{2}$$

where $V(\phi[s])$ means total potential energy obtained by substituting $\phi[s]$ for ϕ in eq 1.

In Figure 7, we plotted the values of $V(s) - V'(s)$ as a function of s, IRC of the retention path. The difference between $V(s)$ and $V'(s)$ cannot be observed in the range of $|s| > 10$; *i.e.*, the reaction coordinate of the migration of silyl group at the early and final stages is congruent with that of the C═CCSi torsion around the *skew* conformer. However, when the reaction proceeds from the reactant, deviation starts suddenly after crossing a border line near $s = \pm 9.5$. In other words, divergence points of the retention path and the torsion path should be located near the points of $s = \pm 9.5$. Using s of the inversion path, quite similar behavior is observed.

We also investigated the change in bond orders along the IRCs concerning important bonds. The bond order B_{AB} between atoms A and B follows as[28]

(28) (a) Mayer, I. *Chem. Phys. Lett.* **1983**, *97*, 270. (b) Mayer, I. *Theor. Chim. Acta* **1985**, *67*, 315. (c) Mayer, I. *Int. J. Quantum Chem.* **1986**, *29*, 73. (d) Mayer, I. *Ibid.* **1986**, *29*, 477.

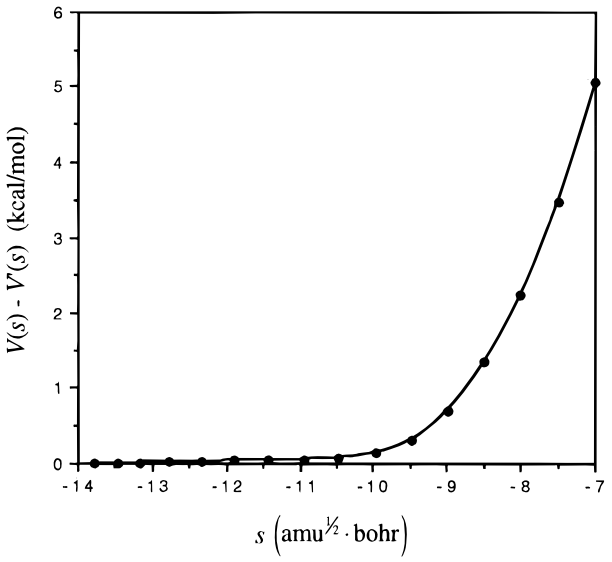

Figure 7. Difference between total potential energy and its C═CCSi torsional segment along the IRC of the retention path.

$$B_{AB} = \sum_{\mu \in A} \sum_{\nu \in B} (\boldsymbol{PS})_{\mu\nu} (\boldsymbol{PS})_{\nu\mu} \tag{3}$$

where $\boldsymbol{P}$ is the density matrix and $\boldsymbol{S}$ is the overlap matrix. As shown in Figure 8, the bond orders B_{12}, B_{14}, B_{23}, and B_{34} are almost constant along the two IRCs in the range $|s| > 10$, and they change monotonically along the IRC in the range $-10 < s < +10$. The change in these bond orders occurs only along the migration path, and the behavior of the silyl group is not only geometrically but also electronically a pure C−C rotation on the C═CCSi torsion path, except for the effect on the $\sigma-\pi$ hyperconjugation. As compared in panels a and b of Figure 8, the changes in B_{12} and B_{23} along the IRC of the inversion path and those of the retention path are quite similar throughout the reaction coordinate, while the changes in B_{14}, B_{24}, and B_{34} are different in the neighborhood of the TSs. For example, $B_{14} = B_{34} = 0.513$ and $B_{24} = 0.160$ for **TS1a**, and $B_{14} = B_{34} = 0.349$ and $B_{24} = 0.341$ for **TS1b**.

In other words, the former has two Si−C "half" bonds, and there is actually no chemical bonding between the silicon atom and the central carbon atom of the allyl fragment (C[2]). On the other hand, the latter has three Si−C "one-third" bonds, and a great stabilization due to the Si−C[2] interaction, which is not seen on the inversion path, is expected. The Si−C[2] interaction on the retention path is looked upon as one of the effective causes of the potential energy of **TS1b** to be lower than that of **TS1a**.

As a result of the change in bond order, the changes of hybridization of atomic orbitals can be understood on each atom. In this system, the carbon atoms which form the C═C double bond are sp^2-hybridized. As to the geometry of the hybridized orbital, moreover, the sp^2 hybridization makes a trigonal planer arrangement and the sp^3 hybridization has a tetrahedral structure. To investigate the formation and dissociation of chemical bonds, let us define and calculate the degrees of nonplanarity (DNP) of the three carbon segments (Δ_1, Δ_2, and Δ_3) and the silyl group (Δ_4), which are written as[29]

$$\Delta_1 = 360° - (\theta_{215} + \theta_{216} + \theta_{516}) \tag{4-1}$$

(29) Korkin, A. A.; Schleyer, P. v. R. *J. Am. Chem. Soc.* **1992**, *114*, 8720.

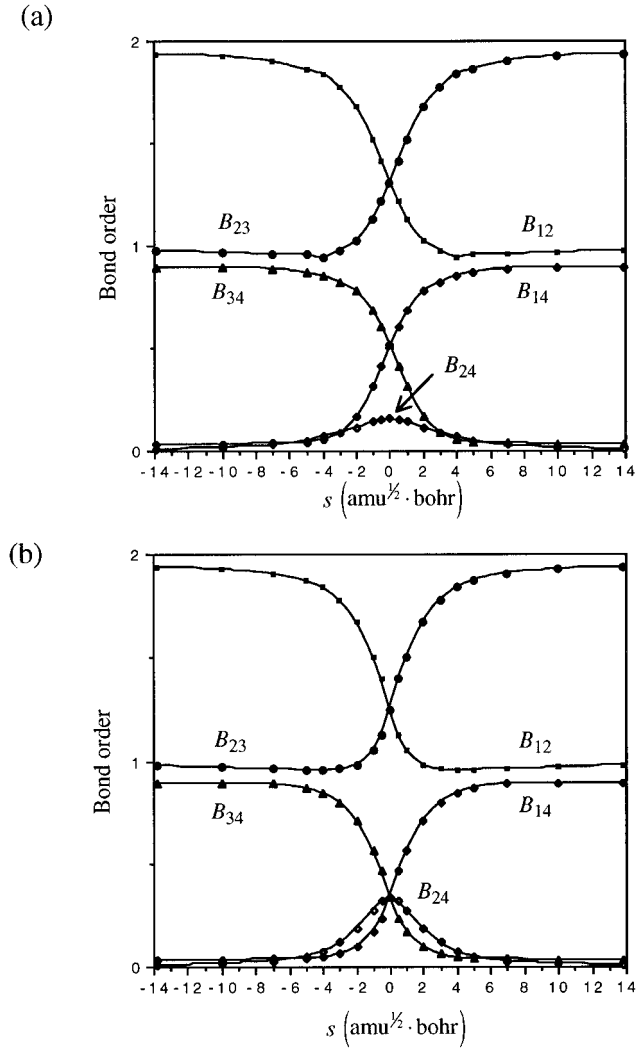

Figure 8. Bond orders along the IRC of (a) inversion and (b) retention paths.

$$\Delta_2 = 360° - (\theta_{123} + \theta_{127} + \theta_{327}) \tag{4-2}$$

$$\Delta_3 = 360° - (\theta_{238} + \theta_{239} + \theta_{839}) \tag{4-3}$$

$$\Delta_4 = 360° - (\theta_{10,4,11} + \theta_{10,4,12} + \theta_{11,4,12}) \tag{4-4}$$

where θ_{ijk} is the bond angle, and i, j, and k are the atomic labels seen in Figure 1.

The value of DNP is 0° in a complete planar arrangement and 31.6° in a complete tetrahedral arrangement. Hence, sp^2 hybridization is realized when the value of DNP is very small, and sp^3 hybridization is realized when the value of DNP is relatively large, near 30°. As shown in Figure 9, as the reaction proceeds, Δ_1 decreases, to show a change from sp^3 hybridization to sp^2 hybridization; Δ_2 does not significantly change, keeping sp^2 hybridization; and Δ_3 increases, indicating a change from sp^2 hybridization to sp^3 hybridization along both the IRCs in the range $-10 < s < +10$.

The values of Δ_4 for the inversion and retention paths are plotted together in Figure 10. One can see from this illustration that the two curves overlap each other in the region $|s| > 5$. That is, the three hydrogen atoms of the silyl group are characteristic of stereochemistry only in the region which is not very far from the TSs, $-5 < s < +5$. When $|s| > 5$, the IRCs of the inversion and retention paths are congruous. Divergence points of another type for the two paths appear in the vicinity of $s = \pm 5$. Δ_4 of the inversion path decreases

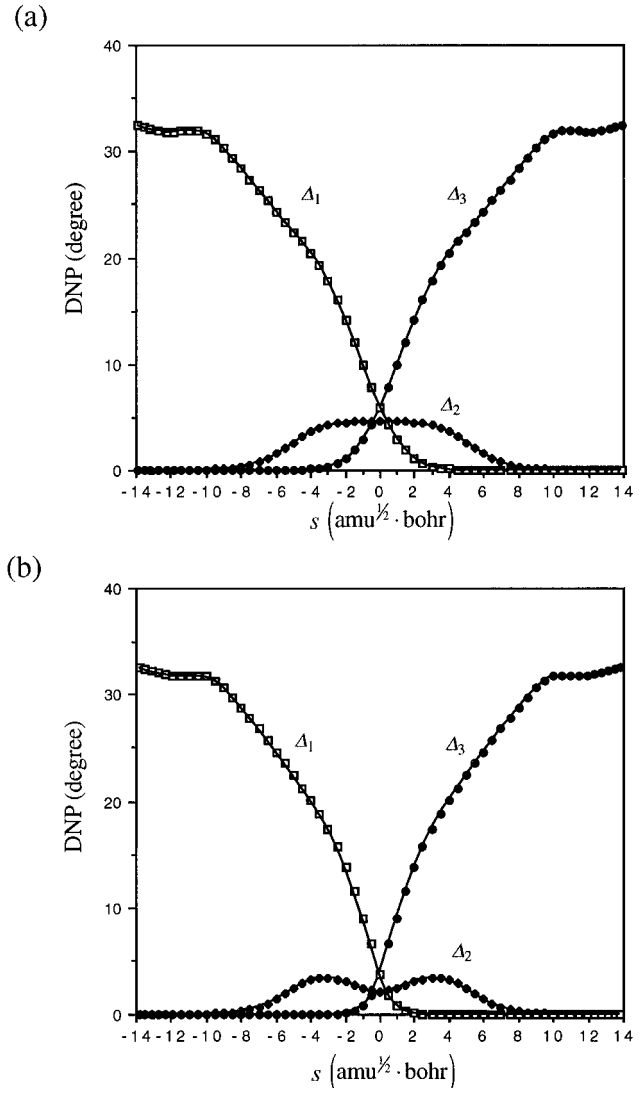

Figure 9. DNPs of the three carbon segments along the IRC of (a) inversion and (b) retention paths.

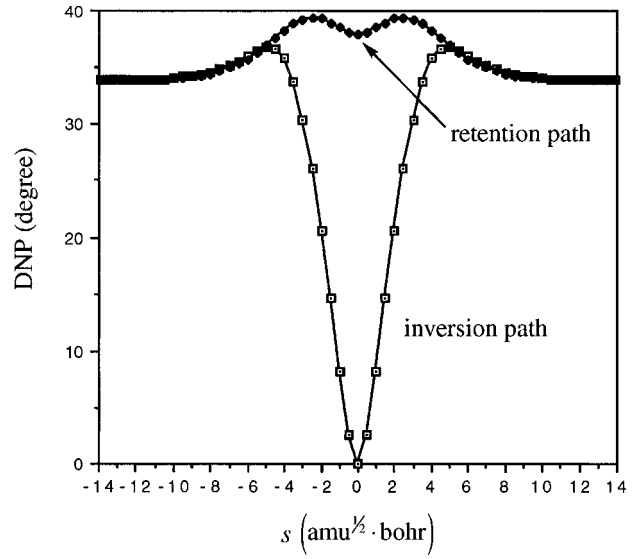

Figure 10. DNPs of the migrating silyl group along the IRCs.

remarkably as the reaction coordinate approaches **TS1a** in which Δ_4 is 0°, and this value increases again as the reaction coordinate goes away from **TS1a**. The silicon atom on the inversion path is almost sp^3-hybridized when $|s| > 5$, while it is sp^2-hybridized near **TS1a**. The change in Δ_4 along the inversion path from the reactant to **TS1a** and that from **TS1a** to the product are not simple, and noteworthy local maximal points, at which Δ_4 is about 3° larger than those of the reactant and product, appear near $s = \pm 4.5$.

On the retention path, the silicon atom is sp^3-hybridized throughout the reaction coordinate. The local maxima of Δ_4 exist near $s = \pm 2.5$ as on the inversion path, but the total profile is quite different from that of the inversion path. Δ_4 of **TS1b** is only 4° larger than that of the reactant and product, in spite of the local minimum. One can see that the profiles of Δ_4 characterize most effectively the difference between the geometries of the migrating silyl group along the inversion and retention paths.

Recently a strain effect due to excessive nonplanarity of silicon was examined for a reaction between substituted allylsilane and carbonyl compound from experimental[2] and theoretical[30] viewpoints. From the viewpoint of local electron-accepting capacitance and acidic hardness[31] expressed in terms of molecular orbitals,[30] the reactivity of substituted allylsilane with aldehyde rises under the existence of strain, due to excessive nonplanarity of silicon atom. This is because both the electron-accepting capacitance and the Lewis acidity of silicon increase as this strain becomes large.[2,30] For allylsilane (**1**), a similar increase in Lewis acidity, which is expected for a nonplanar silyl group, is indispensable in order to go through the TS along the IRC, even on the inversion path.

In Figure 11, the molecular shape and frontier orbitals[32] of **1** are illustrated along the IRCs of the inversion and retention paths. In general, an intramolecular thermal sigmatropic reaction is characterized well by the highest occupied molecular orbital (HOMO).[10] On the inversion path of **1**, the HOMO is composed mainly of the antisymmetric 3p atomic orbital of the migrating silicon atom. It is in phase with the two 2p orbitals of the terminal carbons of allyl along the reaction coordinate in the neighborhood of the TS. From the viewpoint of orbital interactions, the inversion path seems to be more favorable than the retention one.

Moreover, on the retention path, the coefficient of the 3p orbital of the silicon atom in the HOMO is almost 0 in the vicinity of **TS1b**. Thus, the retention path seems to be unfavorable from the viewpoint of orbital interactions. However, our calculations at various levels of theory show that the activation energy of the retention path is lower than that of the inversion path in **1**. In this way, we cannot determine which path is more favorable just from the observation of the HOMOs of the two transition states.

Figure 12 shows the frontier orbitals in **TS1a** and **TS1b**. Let us look at these in order to consider the origin of the lower activation energy on the retention path. The (HOMO−1) of **TS1b** is just like the HOMO of **TS1a**; the 3p orbital of the silicon atom is in phase with the 2p orbitals of the terminal carbons of allyl. As a result, it is greatly stabilized in energy. On the other hand, the (HOMO−1) of **TS1a** is destabilized, due to its out-of-phase character, as seen in Figure 12. Thus, the HOMO and (HOMO−1) are nearly degenerate in **TS1a**. The LUMO and (LUMO+1) are also nearly degenerate. Consequently, the activation energy of the retention path may be lowered compared with that of the inversion path from a simple one-electron picture.

(30) Omoto, K.; Sawada, Y.; Fujimoto, H. *J. Am. Chem. Soc.* **1996**, *118*, 1750.
(31) Fujimoto, H.; Satoh, S. *J. Phys. Chem.* **1994**, *98*, 1436.
(32) (a) Fukui, K.; Yonezawa, T.; Shingu, H. *J. Chem. Phys.* **1952**, *20*, 722. (b) Fukui, K.; Yonezawa, T.; Nagata, C.; Shingu, H. *J. Chem. Phys.* **1954**, *22*, 1433. (c) Fukui, K.; Yonezawa, T.; Nagata, C. *Bull. Chem. Soc. Jpn.* **1954**, *27*, 424.

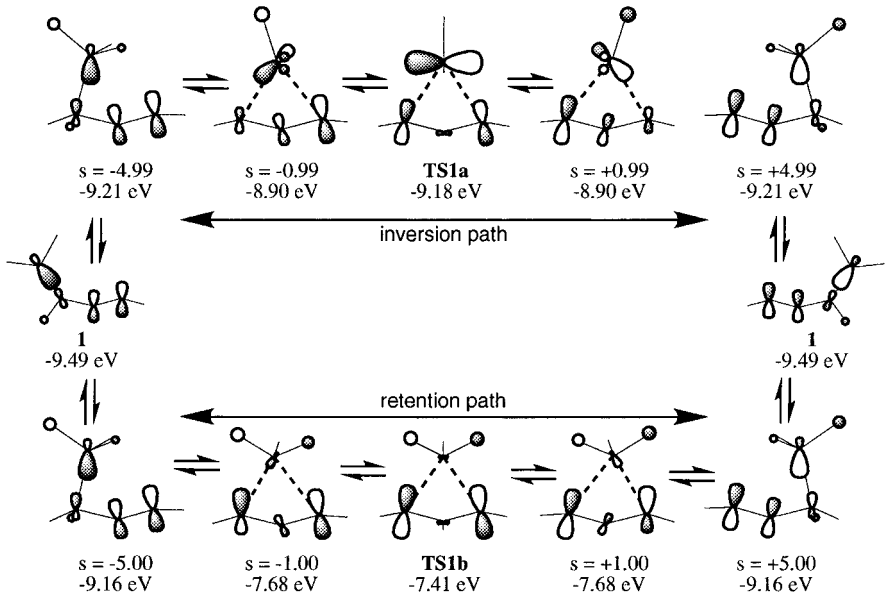

Figure 11. The HOMOs and their energies along the IRCs at the HF/6-31G** level.

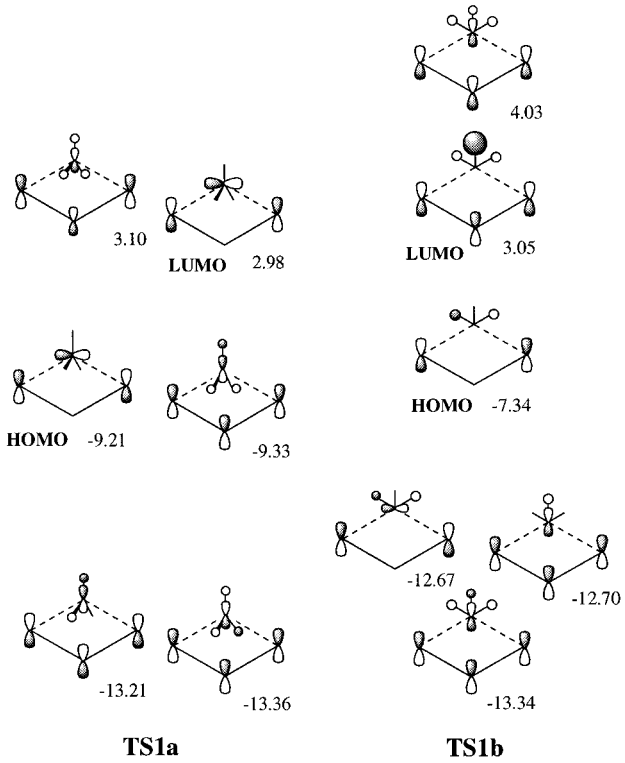

Figure 12. Frontier orbitals at **TS1a** and **TS1b** at the MP2(full)/6-31G** level. Values are the orbital energies.

This situation is quite different in a carbon-based system **2**. The energy separation between HOMO and (HOMO−1) and that between LUMO and (LUMO+1) are large in **TS2a** on the inversion path of **2**. As mentioned above, *ab initio* calculations show that the inversion path is energetically more favored than the retention path in **2**.

Conclusions

The conformational preference and [1,3] sigmatropic silyl shift in the simplest member of allylsilanes, SiC_3H_8 (**1**), has been analyzed using *ab initio* molecular orbital methods. We have confirmed that the $\sigma-\pi$ hyperconjugation effect in **1** is more important than in 1-butene (**2**). In other words, the 3p orbital of the silicon atom in the migrating silyl group makes

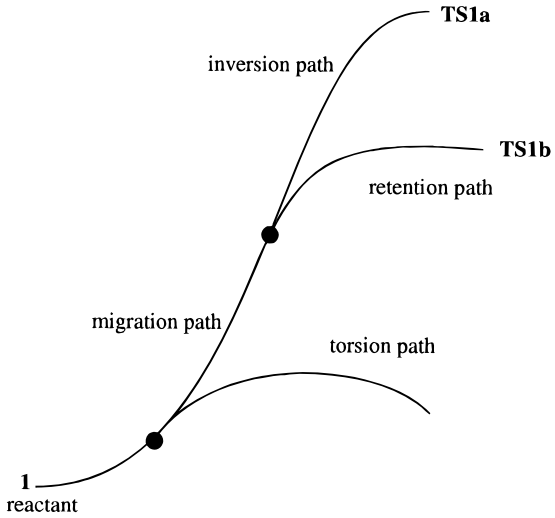

Figure 13. Schematic representation of the reaction paths and divergence points.

an interaction with the terminal 2p orbitals of the allyl fragment more easily than the 2p orbital of the carbon atom in the migrating methyl group.

The activation energy along the retention path was calculated to be lower than that along the inversion path in **1** at various levels of theory, which is in remarkable contrast to the carbon-based system **2**. From the activation energies calculated, the retention path is preferred in **1**. However, from the viewpoint of orbital interactions (W−H rules), the inversion path seems to be more favorable, because the 3p orbital of migrating silyl and the 2p orbitals on the terminal carbon atoms of allyl are in phase. These two effects seem to strongly compete in determining stereoselection of the intramolecular migration of **1**. Since the HOMO and (HOMO−1) are nearly degenerate in the transition state of the inversion path for **1**, the contribution of the HOMO seems less important in this system. In this point our knowledge is clearly still lacking, and the analysis of stereoselection of organosilicon compounds by means of modern X-ray and spectroscopic techniques is of great interest.

In the [1,3] silyl shift, two types of divergence points exist along the reaction path, as indicated in Figure 13. In particular, the electronic state and the vibrational modes in the inversion−retention divergence points would be worthy of notice as the

Scheme 4

information sources concerning which path is preferred for the stereochemistry in silicon compounds. The analysis of this type of divergence points will be discussed elsewhere.

In conclusion, the activation energy along the retention path is approximately 10 kcal/mol lower than that along the inversion path for the [1,3] silyl shift in allylsilane. We have discussed two types of mechanisms for the silyl migration, *i.e.*, (1) energetical control of the retention path and (2) orbital-symmetry control of the inversion path. We think that the retention path is more favorable than the inversion path in the [1,3] silyl shift of allylsilane. This conclusion seems quite reasonable in view of the structures of methyl and silyl radicals indicated in Scheme 4.

According to previous ESR studies[33] and *ab initio* calculations,[34−36] silyl radical takes a pyramidal form, in contrast to methyl radical, which is planar. We showed in Figure 10 that the silicon atom is sp^3-hybridized entirely along the retention path; on the other hand, it is sp^2-hybridized near the TS on the inversion path. Thus, our calculational result that the retention path is more favorable in **1** would be rationalized by the fact that silyl radical has a trigonal pyramidal form.

Acknowledgment. This work was supported by a Grant-in-Aid for Scientific Research from the Ministry of Education, Science and Culture of Japan and by a JSPS Program for Research for the Future. Numerical calculations were performed at the Data Processing Center of Kyoto University, the Supercomputer Laboratory of the Institute for Chemical Research of Kyoto University, the Computer Center of the Tokyo Institute of Technology, and the Institute for Molecular Science.

JA9623525

(33) (a) Morehouse, R. L.; Christiansen, J. J.; Gordy, W. *J. Chem. Phys.* **1966**, *45*, 1751. (b) Jackel, G. S.; Christiansen, J. J.; Gordy, W. *J. Chem. Phys.* **1967**, *47*, 1751.

(34) Selmani, A.; Salahub, D. R. *Chem. Phys. Lett.* **1988**, *146*, 465.

(35) Moc, J.; Rudzinski, J. M.; Ratajczak, H. *Chem. Phys.* **1992**, *159*, 197.

(36) Rodriquez, C. F.; Hopkinson, A. C. *Can. J. Chem.* **1992**, *70*, 2234.